Supplementary Material (ESI) for Chemical Communications

Supporting Information for "Generation of a Solid Brønsted Acid Site in a Chiral Framework"

Michael J. Ingleson, Jorge Perez Barrio, John Bacsa, Calum Dickinson, Hyunsoo Park and Matthew J. Rosseinsky*

INDEX

Experimental Procedures	2 - 4
Crystallography Report (Figures S1 and S2)	5-6
IR Spectra (Figures S3 to S7)	7-9
Thermogravimetric Analysis (Figures S8 to S14)	10-12
EDX analysis (Figures S15 to S18)	13
Guest Uptake Analysis (Figures S19 to S23)	14-15
Powder X-Ray diffraction (Figure S24 to S30)	16-18
SEM pictures (Figures S31 and S32)	19
Simplified Structural schematics/net analysis (Figures S33 to S35)	20-21

Experimental Procedures:

Framework **1** was synthesised according to the published protocol.[1] Unless otherwise stated all other materials were used as received from commercially vendors. All syntheses of the protonated phases and all catalytic reactions were performed under inert atmosphere using rigorously dried solvents. Et_2O and MeOH were dried and degassed using standard methodology (Na/benzophenone for Et_2O and Mg for MeOH) and stored over activated molecular sieves under argon.

Ni(asp)(bipy)$_{0.5}$(HCl)$_{0.9}$(MeOH)$_{0.5}$ (2): A Schlenk flask was charged with **1** (200 mg, 0.75 mmol) and 5 ml of anhydrous diethyl ether. 1 ml (1.2 equivalents per Ni) of 1M HCl in diethyl ether was added to the green suspension by syringe. The suspension was stirred for 18 h filtered and washed repeatedly to yield 210 mgs of light green solid. The degree of phase purity was judged by a combination of powder X-ray diffraction, microanalysis, TG and EDX analysis (see below).
Yield = 88 %
Microanalysis predicted (%) C = 36.0 H = 3.8 N = 8.7. Found (%) C = 36.0, H = 3.8 N = 8.6.
Predicted combined solvent and HCl mass loss = 15.1 %
Observed combined Solvent and HCl mass loss = 14 %
Numerous reactions to produce **2** as a single phase without the two minor impurities phases, **1** and Ni(bipy)Cl_2, were attempted including; using excess HCl, low temperatures (-78°C), shorter reaction times, stepwise HCl addition, substoichiometric HCl, gas phase diffusion of $HCl_{(g)}$, all to no avail. Thus the above synthesis is the optimised that maximises conversion to **2** whilst minimising the two impurities; they are however still detectable by powder X-ray diffraction at very low relative percentages (see pXRD section).

Cu(asp)bipy$_{0.5}$(H$_2$O)$_1$, (3): 44 mg of 4,4′-bipy (0.28 mmol), 48mg $NaHCO_3$ (0.56 mmol), 64mg $Cu(NO_3)_2{\cdot}3H_2O$ (0.28 mmol) and 75 mg aspartic acid (L- or D-) (0.56 mmol) were placed in a 23 ml Teflon lined solvothermal vessel and dissolved in a water/methanol mixture (3ml/3ml). The reaction mixture was heated at 100°C for 18 h (heating period = 2°C/min; cooling period 0.1°C/min). Blue cubic crystals were obtained by filtration and washed with water and methanol.
Solvated microanalysis (%), predicted C = 37.2 H = 3.7 N = 9.6 Cu = 21.8. Found C = 37.1 H = 3.2 N = 9.6 Cu = 21.7
Desolvated microanalysis (%), predicted C = 39.6, H =3.3, N = 10.3. Found = 39.5, H = 3.3, N = 10.3
Yield = 40%
Bulk Chirality 100% (GC)
Predicted solvent Mass Loss = 6.3 %
Observed Solvent Mass = 7 %
Single phase morphology is confirmed by xRPD and SEM (see later sections)

Cu(asp)(bpe)$_{0.5}$(H$_2$O)$_{0.5}$(MeOH)$_{0.5}$ (4): 51.4 mg of 1,2-bis(4-pyridyl)ethylene (0.28 mmol), 48 mg $NaHCO_3$ (0.56 mmol), 64 mg $Cu(NO_3)_2{\cdot}3H_2O$ (0.28 mmol) and 75 mg aspartic acid (L- or D-) (0.56 mmol) were placed in a 23 ml Teflon lined solvothermal vessel and dissolved in a water/methanol mixture (3ml/3ml). The reaction mixture was heated at 100°C for 18 h (heating period = 2°C/min; cooling period 0.1°C/min). Turquoise cubic crystals were obtained by filtration and washed with water and methanol.
Yield = 45%.
Solvated Microanalysis (%) predicted C = 40.6, H = 4.2 N = 9.0 Cu = 20.4. Found C = 40.8 H = 4.1 N = 8.8 Cu = 20.4.
Desolvated microanalysis (%) predicted C = 42.3 H = 3.5 N = 9.8. Found C = 42.5 H = 3.8 N = 9.7.
Bulk Chirality 100% (GC)
Predicted solvent mass loss = 8.2 %
Observed solvent mass loss = 8.4 %
Single phase morphology is confirmed by xRPD and SEM (see later sections)

Cu(L-asp)(bpe)$_{0.5}$(HCl)$_1$(H$_2$O)$_1$ (5) (6 based on D-asp is produced in a fully analogous manner): A Schlenk flask was charged with **4** (325 mg, 1.1 mmol) and 10 ml of degassed/anhydrous ether. 1 ml (0.95 equivalents) of 1M HCl in ether was added to the blue suspension by syringe. The suspension was stirred for 1 hour, the resultant green solid was filtered and washed repeatedly to yield 320mgs of green solid. Phase purity was judged by a combination of powder X-ray diffraction, microanalysis, TG and EDX analysis (see below).
Yield = 89%
Microanalysis predicted (C 35.3 = H = 3.8 N = 8.2) Found C = 35.3, H = 3.7 N = 7.9.
Predicted solvent mass loss = 5 %
Observed solvent mass loss = 4.7 %

Cu(L-asp)(bpe)$_{0.5}$(HCl)$_1$(H$_2$O)$_{0.2}$(propylene oxide)$_{0.2}$: A sample of **5** was desolvated overnight *in-vacuo* ($1x10^{-3}$ torr at 25°C) and suspended in 1 ml propylene oxide for 6 hours. The sample was filtered and air dried at 30°C.
Solvated microanalysis predicted (%) C = 37.8, H = 3.8, N = 8.3. Found (%) C =37.8, H = 3.8, N = 8.3.
Predicted Solvent mass loss = 4.5 %
Observed solvent mass loss by TGA = 4.5 %

Catalysis:

Typical catalytic epoxide methanolysis: 10 mgs of solid catalyst is loaded into a Schlenk flask and desolvated overnight at 25°C and $1x10^{-3}$ torr. The resultant solid is suspended in dried and degassed MeOH and 30 µl of the desired epoxide reagent is added by microlitre syringe under inert atmosphere and the vessel sealed. After stirring for 48 hours the material is filtered and the solid washed with MeOH, all MeOH portions are combined and yield and e.e are determined using a combination of LIPODEX®-E and alpha-DEX™-120 chiral columns directly with the unfunctionalised methoxy-alcohols.

Catalysed methanolysis of propylene oxide (PO).

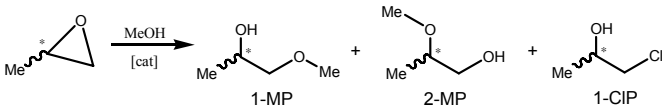

Table 1. Catalysis results for the methanolysis of propylene oxide

Cat[a]	Reactant/T(°C) conditions	Yield (%)	%1MP (ee)[d]	%2MP (ee)	%1ClP (ee)	TOF (mol^{-1} day^{-1})
2	RacPO[b] 25°C	2	51(0)	40(0)	9(0)	0.1
4	RacPO 25°C	0	0	0	0	0
5	RacPO 25°C Run 1	21	50(0)	45(0)	5(0)	1.1
5	RacPO 25°C Run 2	19	56(0)	40(0)	4(0)	1.0
5	RacPO 25°C Run 3	14	52(0)	42(0)	6(0)	0.8
5	s-PO[c] 25°C	22	52(100)	42(100)	6(100)	1.2
5	RacPO 60°C	45	49(0)	47(0)	4(0)	3.2
HCl[e]	RacPO 25°C	42	43(0)	41(0)	16(0)	1.8

[a] All solid catalysts activated overnight *invacuo* and then suspended in 5ml dry MeOH under argon followed by addition of 30µlof epoxide. [b] RacPO = racemic propylene oxide [c] s-PO = enantiopure (>98%) *s*-propylene oxide [d] conversions were determined by GC whilst e.e's were assessed using chiral GC and are fully reproducible [e] 0.05 ml of 1M HCl in diethyl ether is used as the catalyst here in 5 ml dry MeOh as per the framework catalyzed reactions.

A number of noteworthy points can be drawn from the catalysis studies; firstly in addition to producing the expected products, 1-MP and 2-MP (see figure), a third pair of enantiomers is observed at low quantity. These are assigned unambiguously as *R* and *S* 1-chloro-propan-2-ol (1-ClP), no significant amount (< 2 % of total observed products) of 2-chloro-propan-1-ol is detected (by GC using commercially available materials). The production of 1-ClP is not unexpected as Cl^- can compete with MeOH as the attacking nucleophile. It is noteworthy that the yield of 1-ClP using **5** is significantly lower than that observed by catalysis with homogeneous HCl (*ca*. 6 % using **5** to 16 % using HCl); confirming that the active species in catalysis using **5** is not solution phase HCl. The formation of 1-ClP has the effect of gradually reducing the acid content in **5** (confirmed by EDX of post catalysis **5** with a Cu/Cl ratio >1), a direct consequence of this is a slow reduction in the observed activity (Table 1). We reiterate that depletion is not due to loss as HCl, established by supernatant catalysis testing and attempts at extracting HCl using neat MeOH both failing. As expected for acid catalysis the product selectivity using **5** favours 1-MP.[2] All three products are produced effectively racemically, with chirality controlled by the starting propylene oxide enantiomer .Use of *S*-propylene oxide resulted in 100% ee *R* products, confirming the expected inversion ring-opening[3] mechanism and the absence of any racemisation steps during the catalysis. The lack of any enantioselective adsorption from *rac*-propylene oxide by **5** is not surprising given that a precise matching to the geometry of the pores is required to generate any significant ee in sorption by $Ni(asp)bipy_{0.5}$.[1] An analogous attempt using the larger racemic *trans*-2,3-epoxybutane (see below) equally resulted in a racemic mixture of the expected ring opened products; again no enantioselective reagent adsorption is observed. The TOFs observed for **5** are only marginally less than that for homogeneous HCl (*ca.* 1 $mol^{-1}day^{-1}$ for **5** compared to homogeneous HCl 2 $mol^{-1}day^{-1}$), and considering the slow rate of reactant adsorption observed combined with possible product inhibition (the bulkier products can be expected to diffuse more slowly out of the material) the heterogeneous catalytic activity of **5** is closely comparable with homogeneous HCl..

Catalysis on the racemic compound trans-2,3-epoxy-butane using 5 and 6:

		Chriality of 3-methoxy-2-butanol							
Reagent	Yield	R,R	S,S	R,S	S,R	Chlorine containing products	Duration	TOF day-1	Catalyst
trans-2,3-epoxybutane	39	-	-	51.7	48.3	0	2d	2.27	Framework 5
trans-2,3-epoxybutane	41.1	-	-	51.9	48.1	0	2d	2.4	Framework 5
trans-2,3-epoxybutane	48.5	-	-	51.1	48.9	0	2d	2.83	Framework 6

Catalysis on the *meso* complex cis-2,3-epoxybutane: All catalyst runs were performed using the standard protocol described above. For the two runs catalyzed by homogeneous acid the epoxide is dissolved in dry methanol and then the amount of acid is added by microlitre syringe under inert atmosphere. It is important to highlight the vastly different selectivity observed using HCl as the catalyst – this led to significant (32 %) of the product being 3-chloro-butan-2-ol. Catalysis with **5** (or **6**) resulted in effectively zero 3-chloro-butan-2-ol (less than 1 %).

Methanolysis of cis-2,3-epoxybutane

Yield	3-methoxy-2-butanol	3-chloro-butan-2-ol	ee	TOF day-1	Catalyst
59	100	0	10	4.8	5
65	100	0	-6	4.7	6
30	100	0	17	2.6	5
32	100	0	-13	2.7	6
100	68.4	31.6	0.5	-	0.05ml of HCl 1M in Ether
100	100	0	1.8	-	H_2SO_4

The negative sign for the ee indicate the opposite enantiomer is in excess as expected on moving from L to D. The

Conditions for Catalysis by the unprotonated material, 4: 10 mgs of **4** was loaded into a Schlenk flask and desolvated overnight at 25 °C and 1 $x10^{-3}$ torr. Under inert atmosphere the solid is then suspended in dried and degassed MeOH and 30µl of racemic propylene oxide added by microlitre syringe. After stirring for 48 hours the solid is filtered off and the solid washed with MeOH, all MeOH portions are combined with the initial filtrate and yield of ring opened products determined by GC with an alpha-DEX^{TM}-120 chiral column, which revealed only rac-propylene oxide.

Catalysis by impurity phase "Cu(bpe)Cl_2": 'Cu(bpe)Cl_2' used for the catalysis testing was synthesized in the following manner: 100mgs of **4** is loaded into a Schlenk flask and suspended in Et_2O. 0.66 ml of 1M HCl in ether (2 equivalents) is added to the blue suspension of **4** by syringe, the Schlenk flask is then sealed and stirred for 18 hours resulting in a colour change from a blue to a brown suspension. The solid is filtered and washed with Et_2O and then MeOH, on methanol washing the solid rapidly changed colour from brown to green, the solid is then dried in air. The powder pattern (see powder X-ray diffraction patterns later in the supporting info.) reveals no **4** or **5** is present and correlates completely with the minor impurity phase observed in the synthesis of **4**. 10 mgs of this solid is transferred to a Schlenk flask and suspended in 5 ml of MeOH, 30 µl of rac-propylene oxide is added via microlitre syringe, the flask sealed and the mixture stirred for 48 hours. The suspension is filtered, washed with MeOH, all MeOH aliquots combined with the initial filtrate and yield of ring opened products determined by GC with an alpha-DEX^{TM}-120 chiral column, which revealed only rac-propylene oxide.

Determination of the bulk chirality of the frameworks:
Firstly, the aspartic acid needs to be extracted from the bulk material, and is done so by adding 1M NaOH (4 ml) to the framework (~ 30 mg) and removing the resulting precipitate by filtration. The addition of NaOH to the framework results in the precipitation of insoluble $Ni(OH)_2$ and the 4,4'-bipyridyl linking ligands which are also insoluble in basic aqueous solution. Removal of the solids leaves disodium-aspartate in the filtrate. The filtrate is neutralised by the addition of 1M HCl and the aqueous solution removed by rotary evaporation. The resulting white solid is a mixture of aspartic acid (^{1}H NMR) and NaCl (generated by the neutralisation step) as confirmed by elemental analysis. Once the aspartic acid has been recovered from the bulk framework sample it is necessary to derivatise this prior to GC analysis. The carboxylic acid groups are first converted to methyl esters by heating in MeOH (4ml) and HCl (4N, 1ml) in a 20 ml round-bottom flask equipped with a condenser for 4 hours. The primary amine is transformed into an amide by reaction with TFA (0.5 ml in 5 ml DCM, RT overnight) as outlined for the diol derivatisation. The NaCl present in the mixture does not interfere with either of the two steps of the derivatisation procedure and is not removed until the very end when the Asp(OMe/TFA) derivative is dissolved in DCM and the NaCl is simply filtered off. The solution concentration for GC analysis is 0.5% (w/v) Asp(OMe/TFA) in DCM, and is carried out using a Lipodex-E capillary-GC column at 120°C.

Crystallography

Refinement Report $Cu_2(C_{12}H_{10}N_2)(C_4H_5NO_4)_2(CH_4O)_2(H_2O)_2$ 4

The unit cell of **4** is pseudo-orthorhombic, but with a much lower R-int value for the monoclinic cell, and systematic absences that were not consistent with orthorhombic metric symmetry. Therefore monoclinic symmetry was selected, and the final cell constants obtained from least-squares refinement of 2614 reflections, with a = 6.644(1), b = 24.1942(3) Å, c = 7.900(1) Å and β = 91.713(2)º. Monoclinic structures that emulate orthorhombic symmetry, are typically twinned, the second domain is related to the first by a 180º rotation, and this extra rotation results in approximate 4-fold symmetry. These crystals appeared to be twinned under polarised light, but the crystal chosen for the analysis did not show obvious macroscopic features of twinning. Test for twinning were carried out, and the case where the second domain is rotated 180º from the first about the *c*-axis, gave the best results (reduced the R-value the most). This structure refined with an absolute structure parameter that deviated substantially from 0 (0.12(2)). Therefore this structure was refined as a combination of a racemic and rotation twin. In previous work on similar compounds the crystals were shown to be twinned racemically.

The multi-scan absorption correction performed by SADABS is based on comparisons of Friedel opposites and these may be non-equivalent due to overlapping reflections from unresolved twinning. Therefore a face-indexed absorption correction (in SADABS) was applied. The crystal faces were indexed, and distances measured using the SMART software.

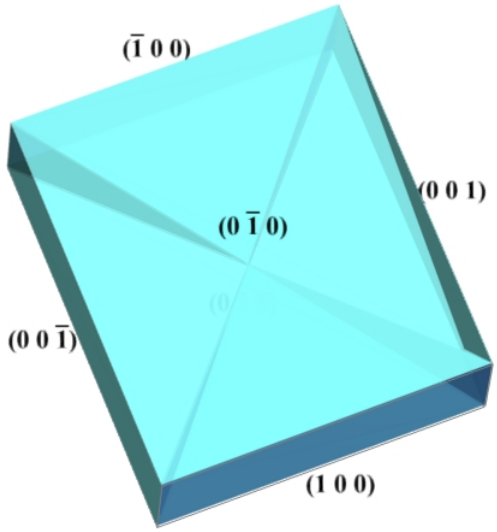

FIGURE S1: Schematic displaying the indexing of each crystal face.

The hydrogen atoms attached to N atoms were located from difference electron density maps and were refined with the N-H and H-H distances restrained. All other hydrogens were refined in a riding mode with values of U_{eq} that were 1.2 times the U_{eq} for the heavy atoms to which they were bonded. It is apparent from the X-ray diffraction results that the porous channels in the crystal contain methanol and water molecules, but also that these channels are half empty. They are weakly held and show up as diffuse electron density corresponding to disordered solvent molecules (methanol molecules and water molecules whose populations refined to approximately 50% full-occupancy). The values refined to 2 water molecules and 2 methanol molecules for each formula unit. TG and CHN analysis confirmed this formulation. TG and CHN analysis confirmed this formulation. The SQUEEZE routine in PLATON (Spek, 2003) was used to remove the contributions of the disordered solvent from diffraction intensities in order to improve the refinement of ordered parts within the structure. (SQUEEZE details are appended to the CIF).
Refinement of F^2 against ALL reflections. The weighted R-factor wR and goodness of fit S are based on F^2, conventional R-factors R are based on F, with F set to zero for negative F^2. The threshold expression of $F^2 > 2\text{sigma}(F^2)$ is used only for calculating R-factors(gt) etc. and is not relevant to the choice of reflections for refinement. R-factors based on F^2 are statistically about twice as large as those based on F, and R- factors based on ALL data will be even larger.

Crystallographic details of the structure of **3** and **4** at 150K have been deposited at CCDC with the following reference numbers:
CCDC- 662350 (**3**)
CCDC-662349 (**4**)

Crystal data for **4**: $C_{22}H_{32}Cu_2N_4O_{12}$, $M = 671.60$, blue pinacoid with 6 faces, $0.20 \times 0.15 \times 0.05$ mm^3, monoclinic, space group $P2_1$ (No. 4), $a = 6.6444(9)$, $b = 24.942(3)$, $c = 7.9004(11)$ Å, $\beta = 91.713(2)°$, $V = 1308.7(3)$ Å^3, $Z = 2$, $D_c = 1.704$ g/cm^3, $F_{000} = 692$, MoKα radiation, $\lambda = 0.71073$ Å, $T = 110(2)$K, $2\theta_{max} = 55.0°$, 6223 reflections collected, 5161 unique ($R_{int} = 0.0208$). Final *GooF* = 1.085, *R1* = 0.0511, *wR2* = 0.1118, *R* indices based on 4806 reflections with I >2sigma(I) (refinement on F^2), 325 parameters, 6 restraints. Lp and absorption corrections applied, $\mu = 1.697$ mm^{-1}. Absolute structure parameter = 0.00 (Flack, H. D. *Acta Cryst*. **1983**, *A39*, 876-881).

Crystal data for **3**: $C_{18}H_{18}Cu_2N_4O_8$, M = 545.45, blue pinacoid, 0.15 x 0.14 x 0.04 mm^3, orthorhombic space group $P2_12_12$, a = 21.424(6), b = 6.897(2), c = 7.800(2) Å, V = 1152.5(6) Å^3, Z = 2, $D_c = 1.572$ g/cm^3, $F_{000} = 552$, MoKα, λ = 0.71073 Å, T = 110(2) K, $2\theta_{max} = 53.4$ °, 5499 reflections collected, 2108 unique ($R_{int} = 0.0710$). Final GooF = 1.060, R1 = 0.0676, wR2 = 0.1488, R indices based on 1706 reflections with I > 2sigma(I)) (refinement on F^2), 175 parameters, 94 restraints. L_p absorption corrections applied, μ = 1.894 mm^{-1}. Absolute structure parameter = 0.09(5) (Flack, H. D. *Acta Cryst.* **1983**, A39, 876-881).

Structure of **3**: Framework **3** is the copper analogue of compound **1** and is closely analogous, equally consisting of M(asp) 2D layers pillared by 4,4′-bipyridyl linkers. The ability to facilely synthesis both **3** and **4** phase pure, demonstrates the potential to develop a family of these materials by simple variation of the rigid pyridyl linker. Figure S2 shows the extended molecular structure of **3** down each axis.

Figure S2: The extended molecular structure of **3** (all hydrogen atoms removed for clarity, both disordered bipy sites shown)

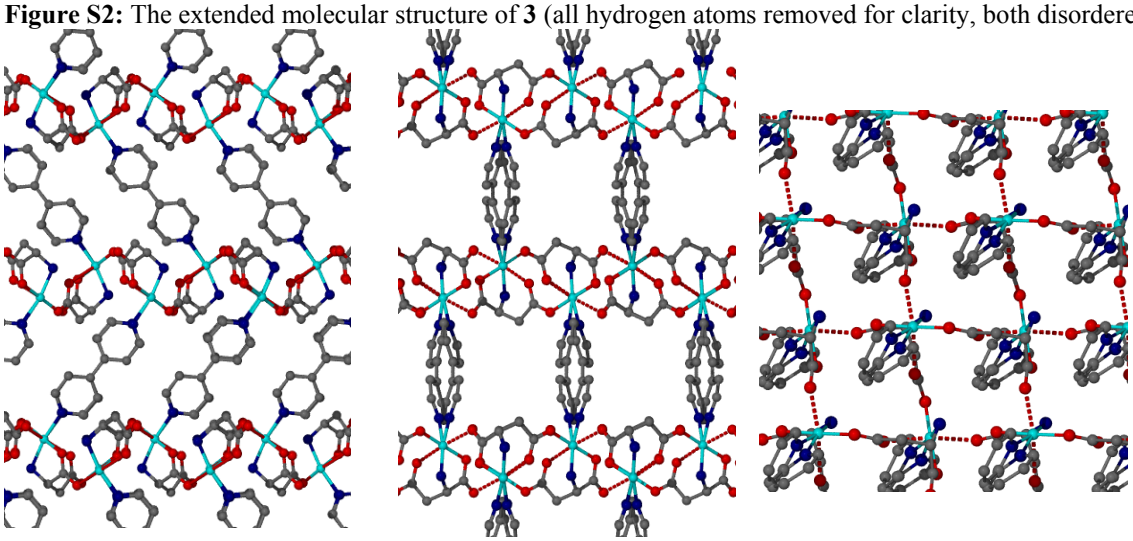

Down a **Down c** **Down b**

InfraRed Spectroscopy:

Fig S3

$Ni(asp)(bipy)_{0.5}(HCl)_{0.9}(MeOH)_{0.5}$ Compound **2**, in KBr. Note the significant shoulder at 1700 and 1718 cm^{-1} attributable to the protonated COOH stretch.

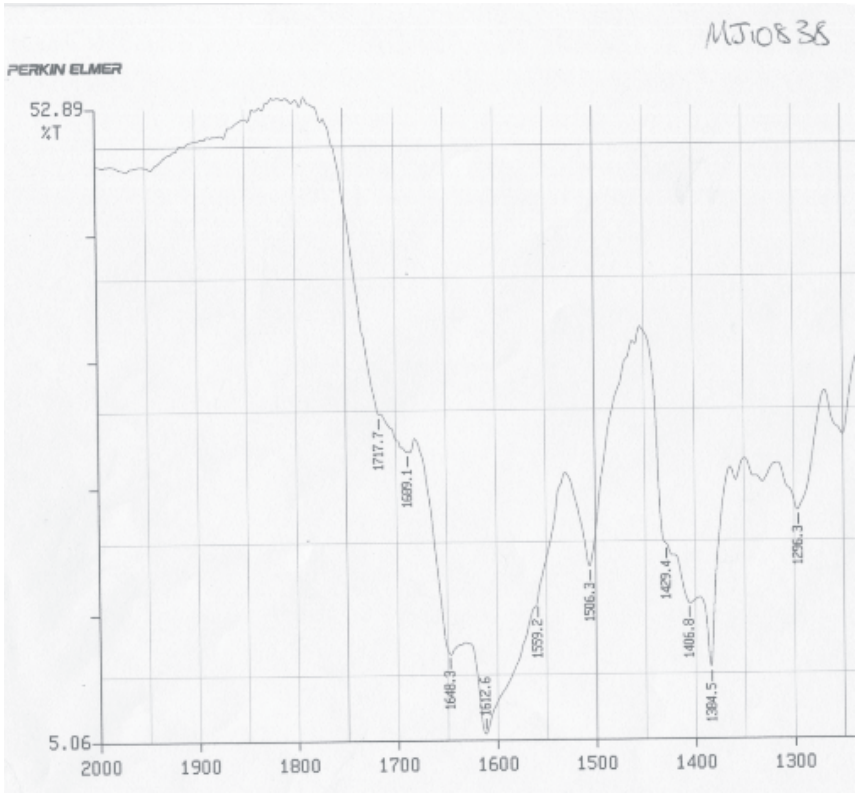

Fig S4: Unprotonated starting material Ni(asp)bipy Framework 1. With no shoulder at 1720 cm^{-1}

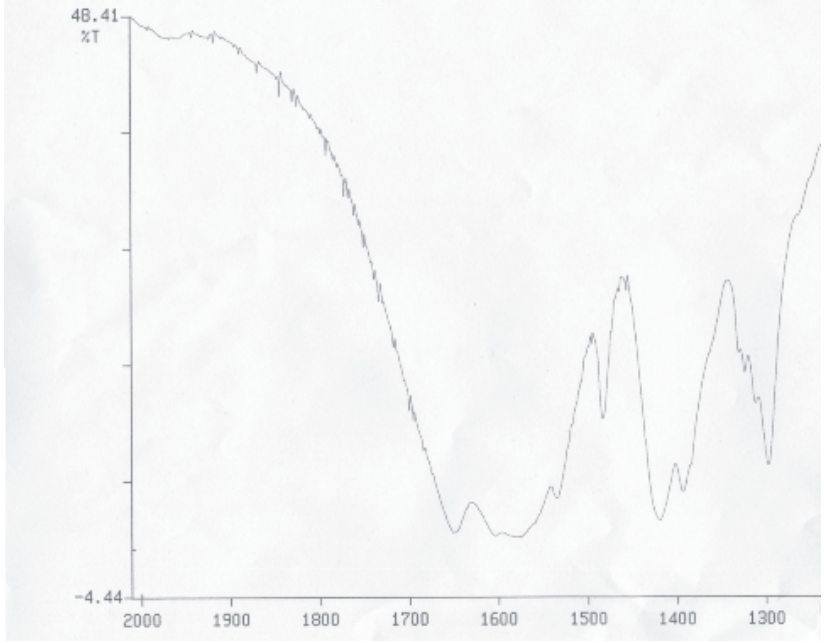

Fig S5
Compound **4** in KBr

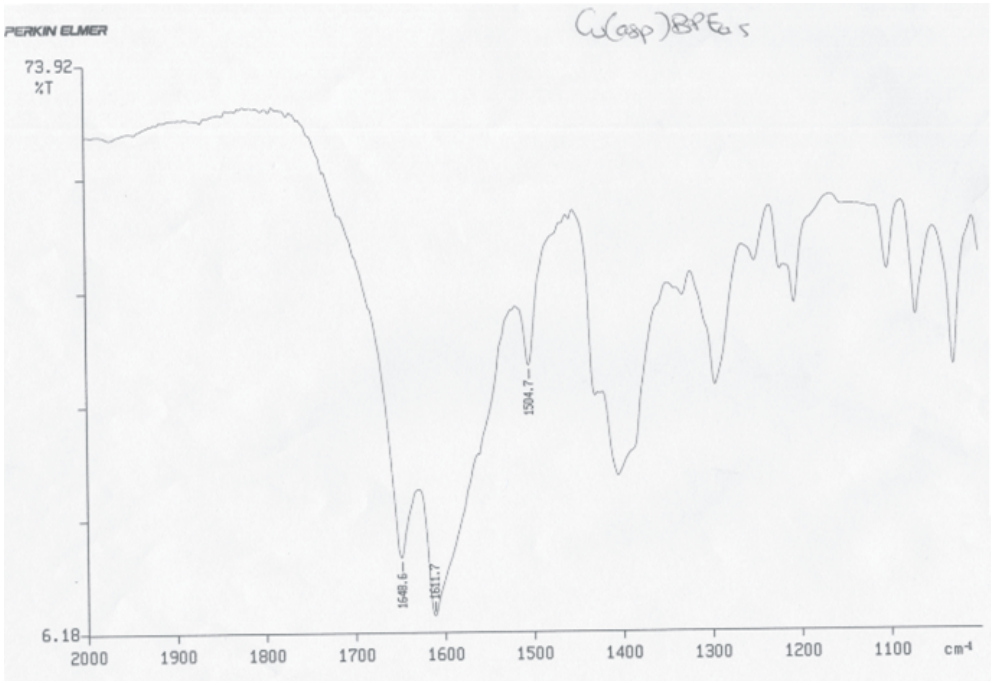

FIG S6
Compound **5** in KBr:

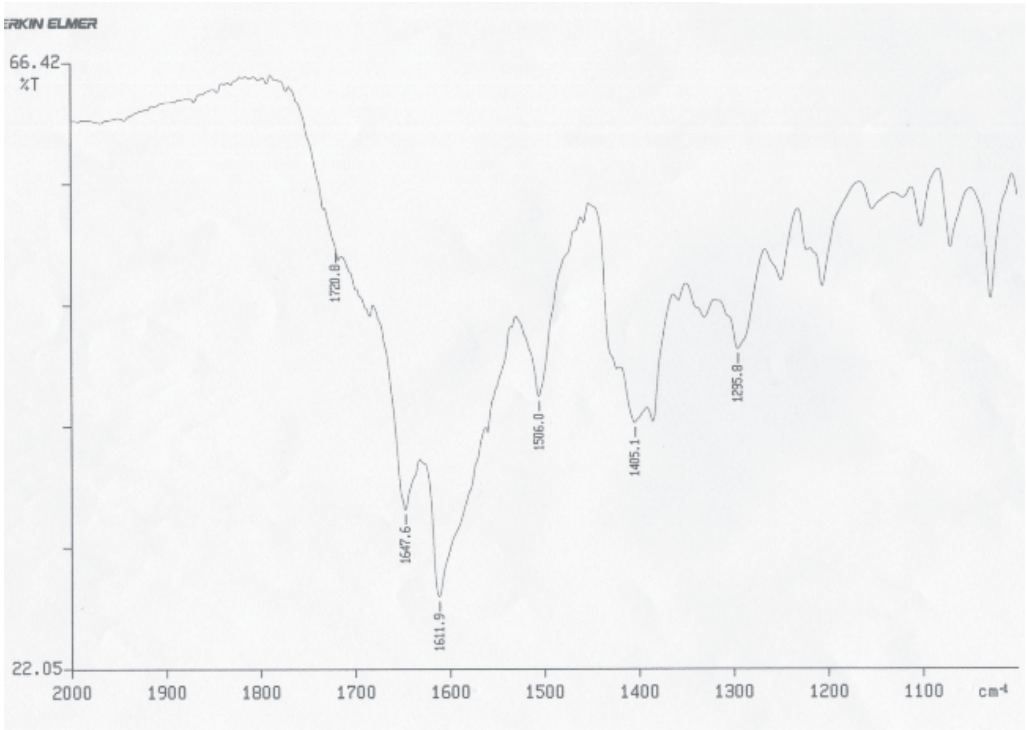

FIG S7

Compound **5** post 3 rounds of catalysis, with bands due to protonated carboxylate still visible at 1720 cm^{-1}, though reduced in intensity at expected by Cl loss due to formation of 1-ClP.

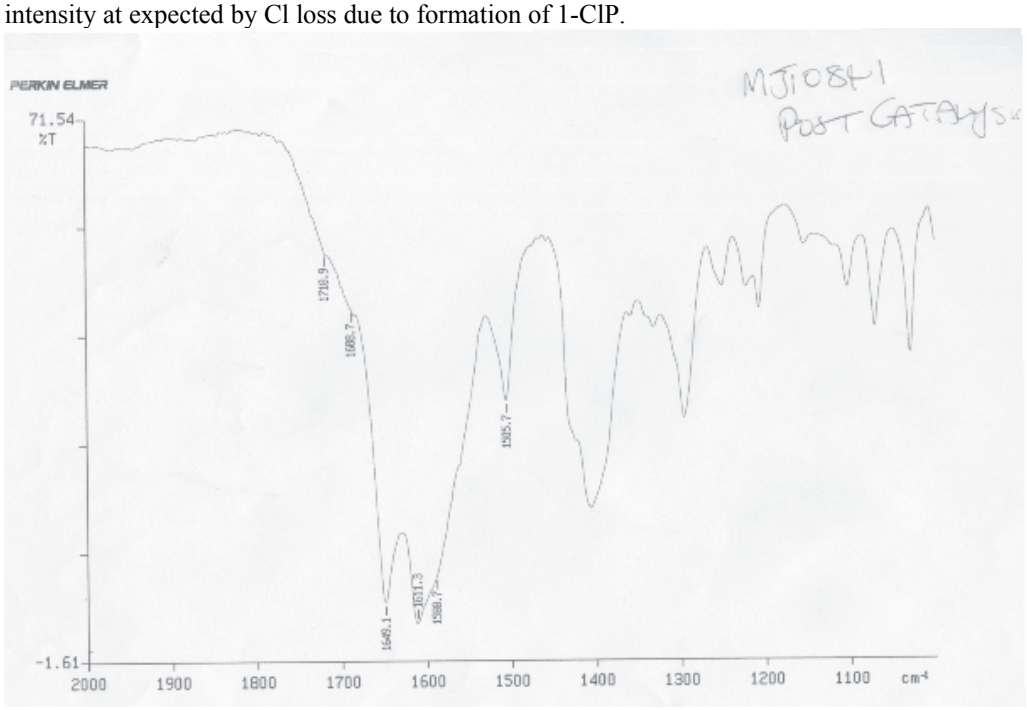

Thermogravimetric analysis

FIG S8

$Ni(asp)(bipy)_{0.5}(HCl)_{0.9}(MeOH)_{0.5}$ (2)

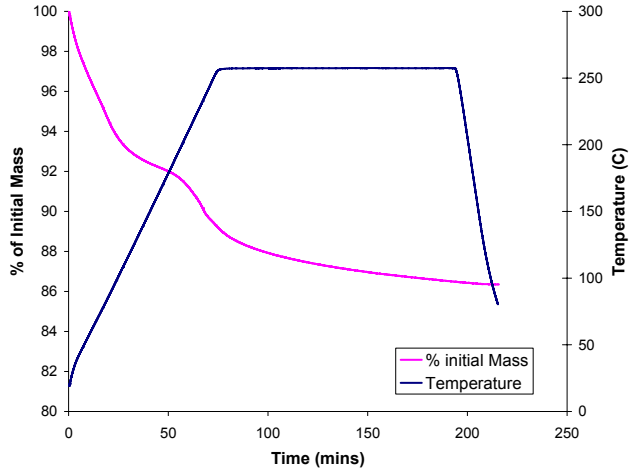

FIG S9

$Cu(asp)bipy_{0.5}(H_2O)_1$, (3):

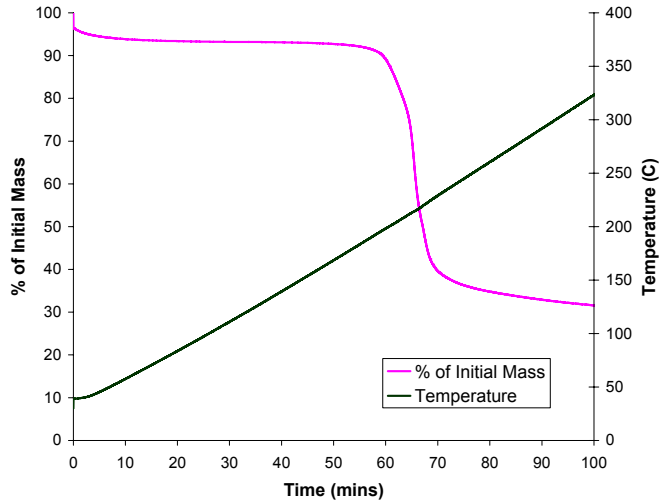

FIG S10

$Cu(asp)(bpe)_{0.5}(H_2O)_{0.5}(MeOH)_{0.5}$ (4):

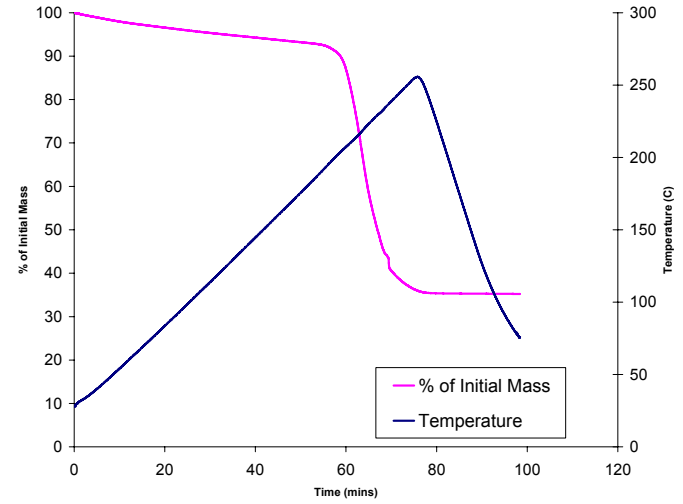

FIG S11

4 desolvated i*nvacuo* overnight at 80°C and 1x10^{-6} torr, suspended in MeOH for 1 h, filtered and dried at 60°C for 1 hour. 6% mass loss before framework decomposition.

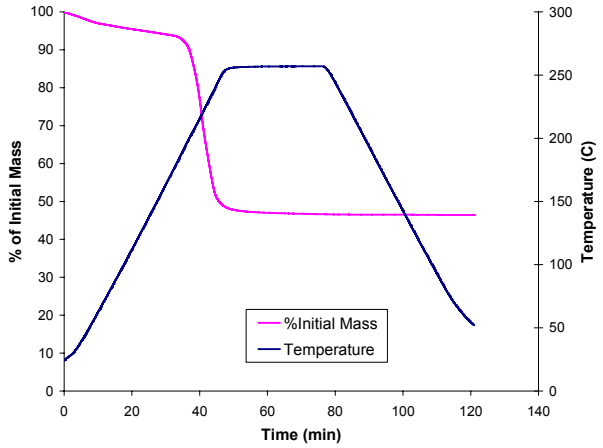

FIG S12

Cu(L-asp)(bpe)$_{0.5}$(HCl)$_1$(H$_2$O)$_1$ (5) (desolvated only no HCl loss)

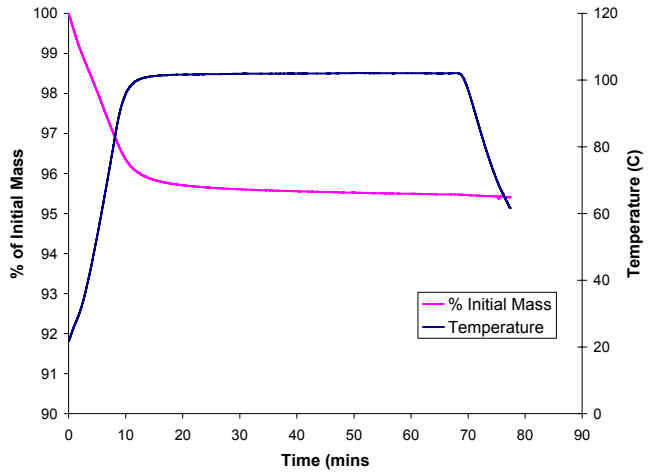

FIG S13

Cu(L-asp)(bpe)$_{0.5}$(HCl)$_1$(H$_2$O)$_{0.2}$(propylene oxide)$_{0.2}$

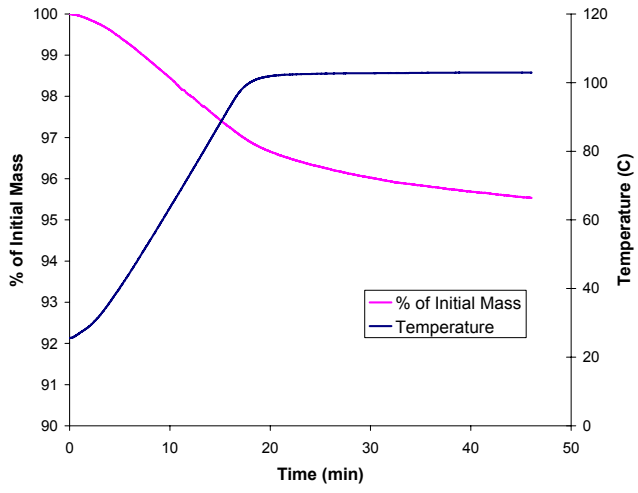

FIG S14
Cu(D-asp)(bpe)$_{0.5}$(HCl)$_1$(H$_2$O)$_1$ (6) (desolvated only no HCl loss)

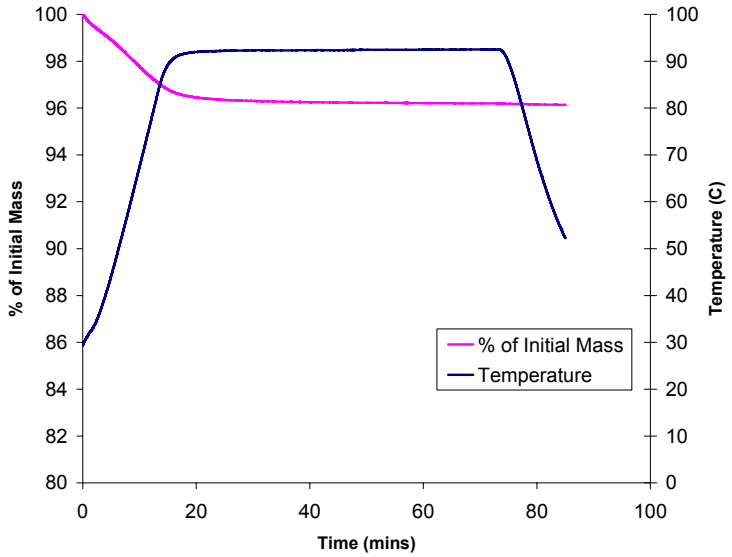

EDX Analyses: Throughout Y axis is the respective elemental percentage ratios.

FIG S15 EDX analysis of as made **2**

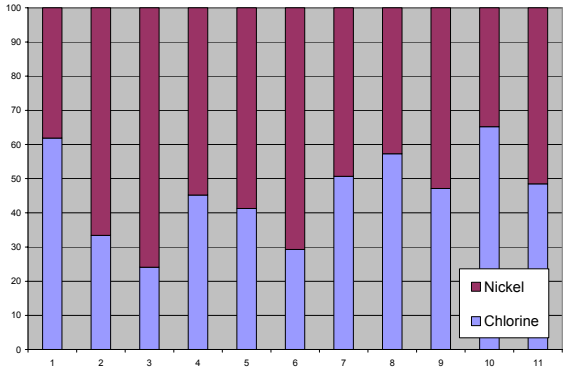

FIG S16

EDX analysis of as made **5**

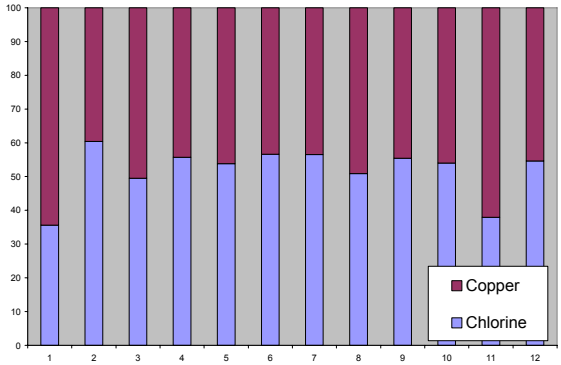

FIG S17

EDX analysis of **5** after 3 sequential catalysis runs.

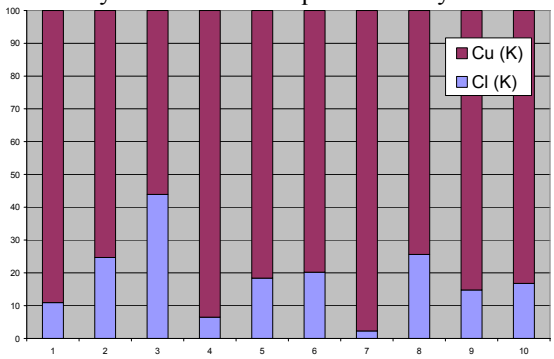

FIG S18

EDX analysis of as made **6**

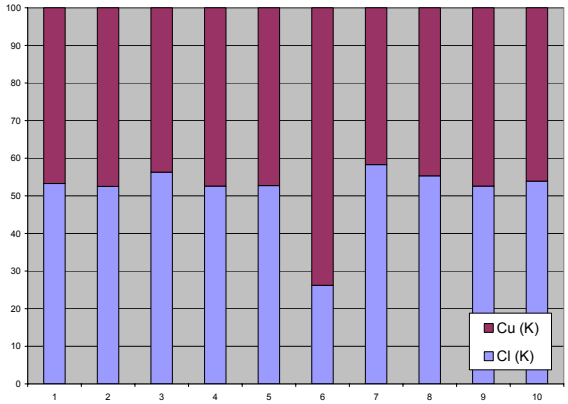

Guest uptake:

Compounds **2**, **4**, **5** and **6** were non porous to conventional gaseous probe molecules, e.g., CO_2 (at 195 and 298 K), N_2 (77 K) and H_2 (77 K). Therefore there porosity was gauged using H_2O and MeOH saturated Argon (saturation achieved by passing the stream of Ar through a bubbler filled with the desired solvent). The samples were measured using a standard TG with 2 gas line inputs, the sample is desolvated by heating under a dry N_2 flow before cooling and gas switched to input 2, the solvent saturated Argon line and held for a set period of time with the gas flow rate at 200ml/minute unless otherwise stated.

FIG S19
MeOH isotherm for compound **2**, displaying very slow uptake of solvent at 200ml/minute flow rate.

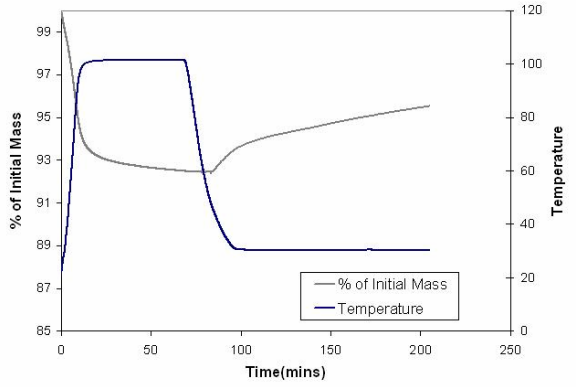

FIG S20
Reversibility in the MeOH isotherm for complex **4**

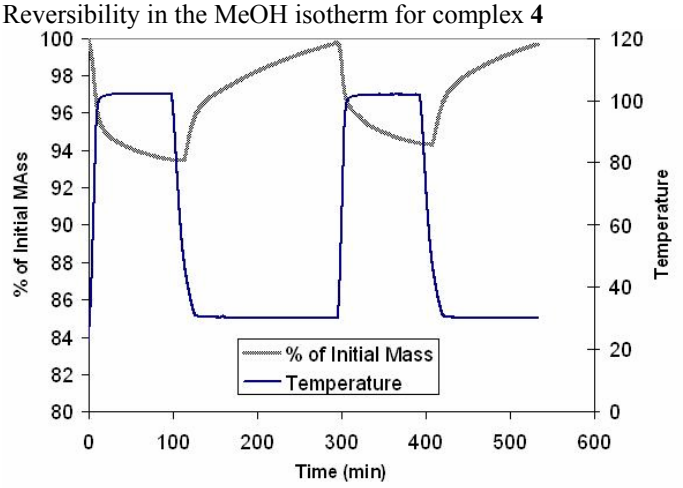

FIG S21
Reversibility in the H_2O Isotherm for Complex **4**

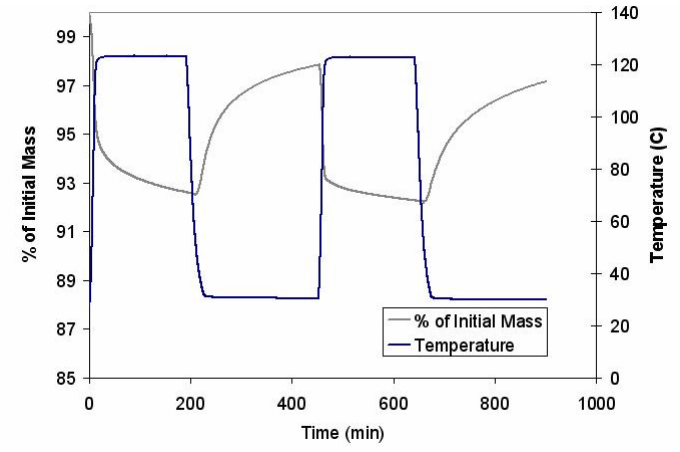

FIG S22
MeOH isotherm for Complex **5**, after 4 hours still not saturated with MeOH, in contrast to starting material **5**.

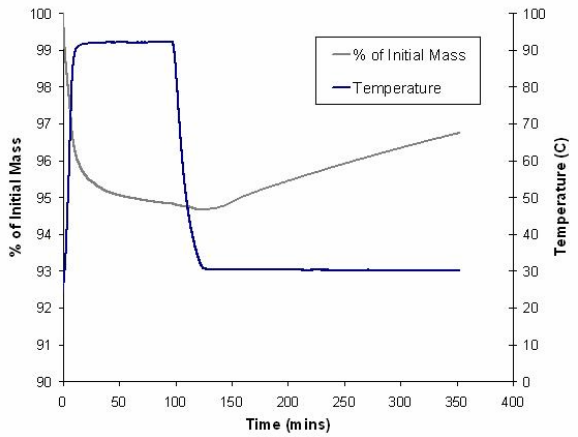

FIG S23
MeOH isotherm at varying gas flow rates for **5**. Under similar conditions (50ml/min Argon saturated with MeOH) **6** showed rapid MeOH uptake. Interestingly, there appears to be a 'gate effect' in the porosity of **5** with a minimum Ar (saturated with MeOH) flow rate required before uptake commences, a minimum flow rate of 200ml/min is required for significant MeOH uptake. This may be necessary to force a displacement of Cl^- from pore window into pore void greatly increasing pore accessibility. This gate-effect may in part explain the observed non-porosity of **5** to CO_2 (at -78°C and 25°C) and H_2 (-196°C) to 1 bar.

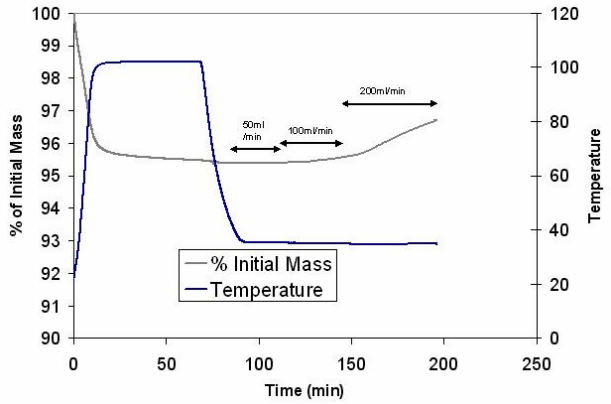

Powder X-Ray Diffraction

FIG S24

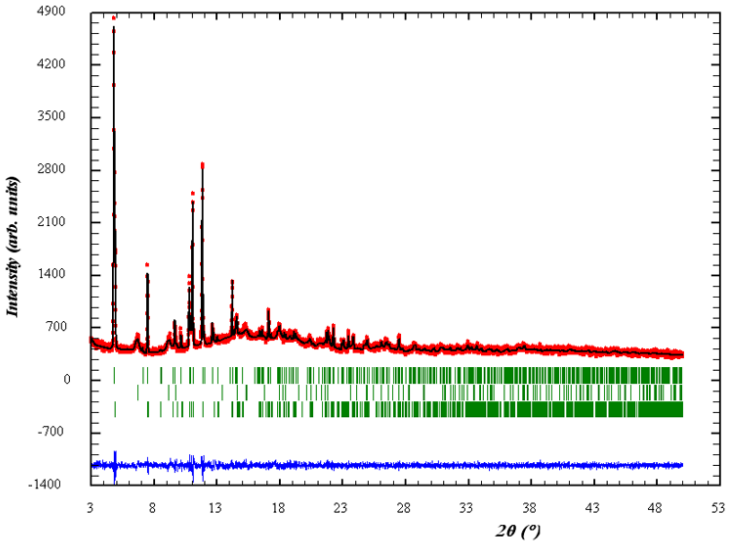

LeBail fit using SRS 9.1 data for Ni(asp)(bipy)$_{0.5}$(HCl)$_{0.9}$(MeOH)$_{0.5}$ (**2**)**:** λ = 0.9588 Å, 2θ = 3.00 – 50.00° stepsize = 0.01°
3 phases present: 1) Major phase – protonated Ni(asp)(bipy)$_{0.5}$ (HCl)$_{0.9}$(MeOH)$_{0.5}$ (**2**), a = 22.769(4) Å b = 6.7588(8) Å c = 7.754(1) Å β = 90.22(1)° V = 1193.2(3) Å^3
2) Minor phase complex **1,** a = 22.369(4) Å b = 6.7607(5) Å c = 7.7410(5) Å β = 90.265(9)° V = 1170.1(2) Å^3
3) Minor phase $NiCl_2$(bipy); a = 11.982(4) Å b = 11.320(4) Å c = 3.583(3) Å V = 486.0(3) Å^3

FIG S25

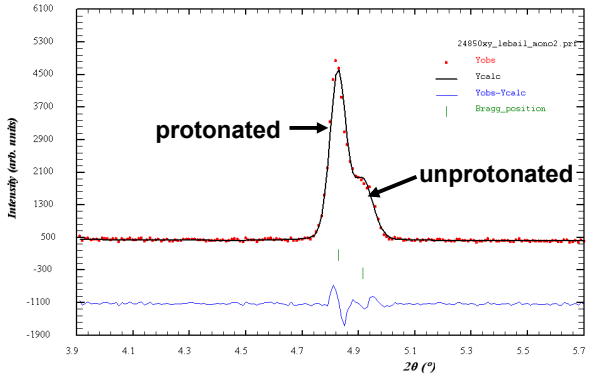

Above, expanded lowest angle peak of **2** showing the combination of protonated and non-protonated phases clearly distinguishable

FIG S26

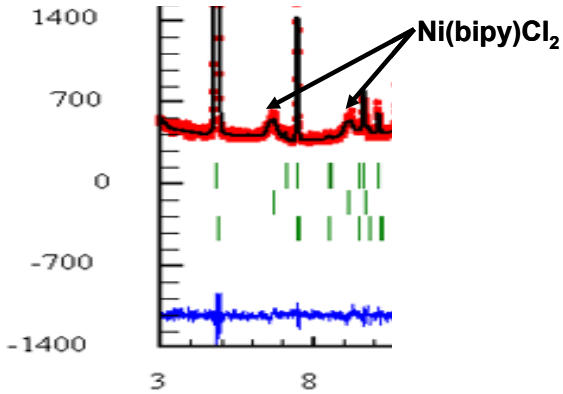

Above, highlighting the two lowest angle broad diffraction peaks for $Ni(bipy)Cl_2$
The reduced crystallinity inherent in **2** post acid-treatment has frustrated attempts at a successful *ab-initio* structural solution from powder XRD data.

FIG S27:
Cu(asp)bipy$_{0.5}$(guests), (**3**):

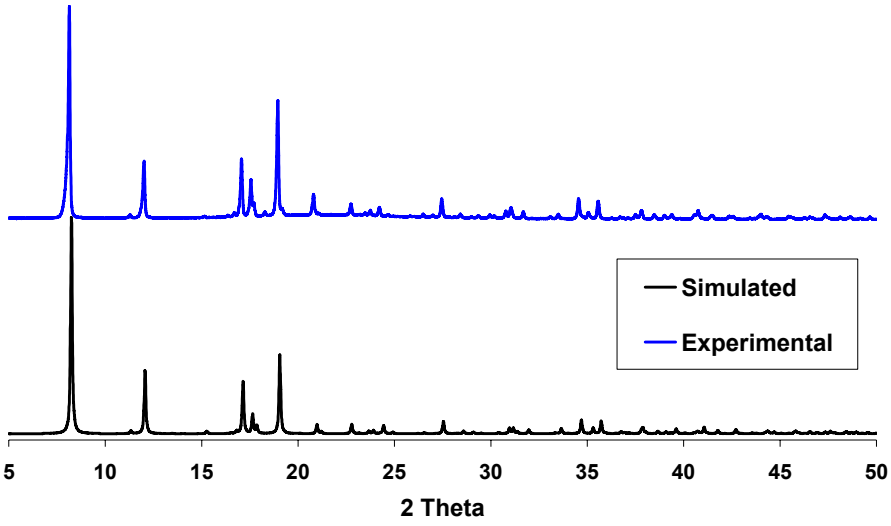

FIG S28
Cu(asp)bpe$_{0.5}$(guests) (**4**).

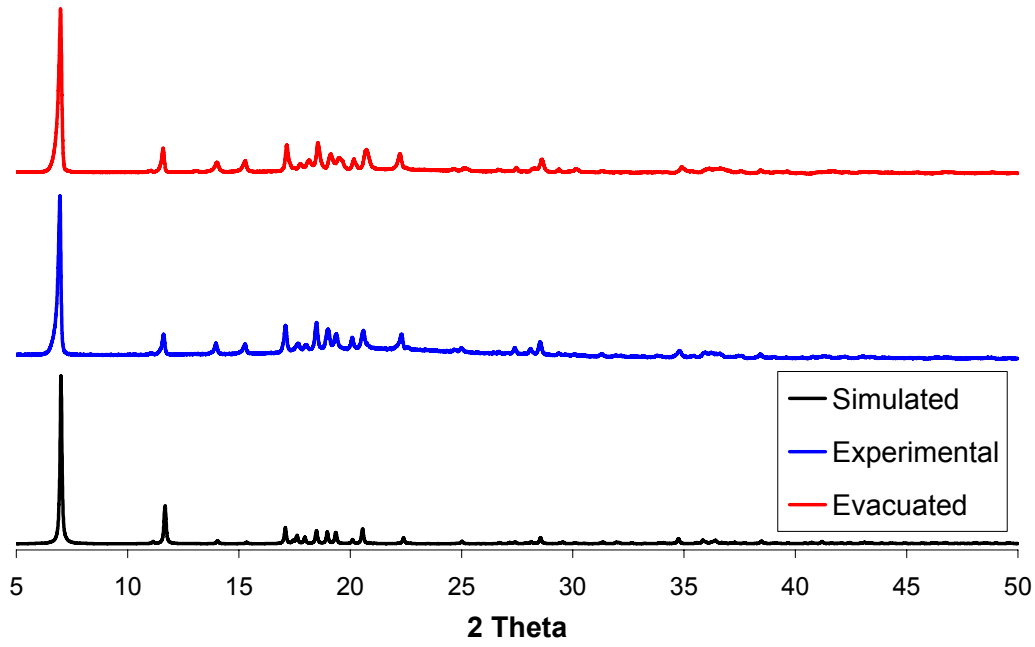

FIG S29:
Cu(asp)bpe$_{0.5}$, simulated (black), before protonation (**4, red**) and after protonation (**5, blue**). Broad peaks in the protonated material tentatively assigned as Cu(bpe)Cl$_2$ by comparison to the Ni analogues.

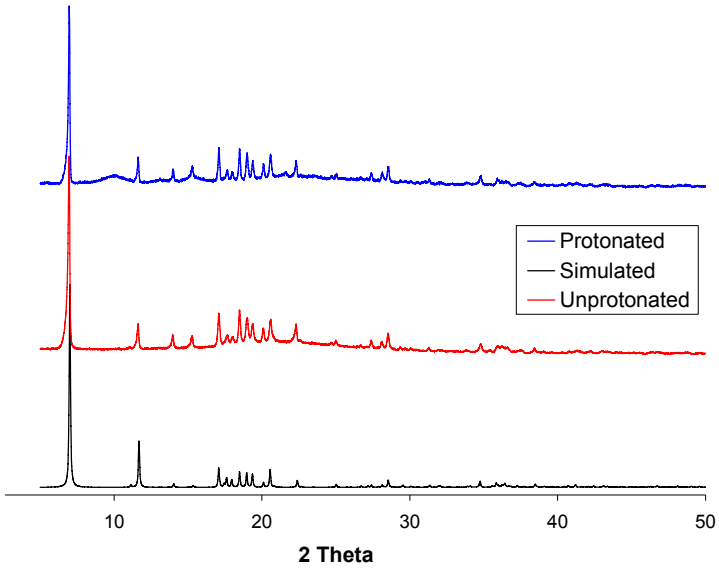

FIG S30:
Below the observed powder pattern on the reaction of Cu(asp)bpe$_{0.5}$ with 2 equivalents of HCl in Et$_2$O, the observed crystalline phase is tentatively assigned as Cu(bpe)Cl$_2$.

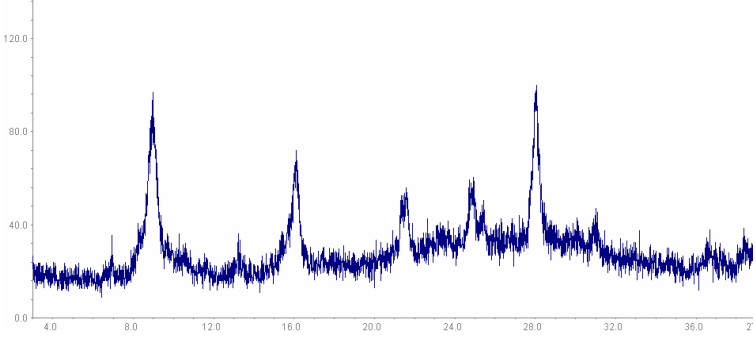

SEM Pictures:

FIG S31
Cu(asp)bipy$_{0.5}$ (3):

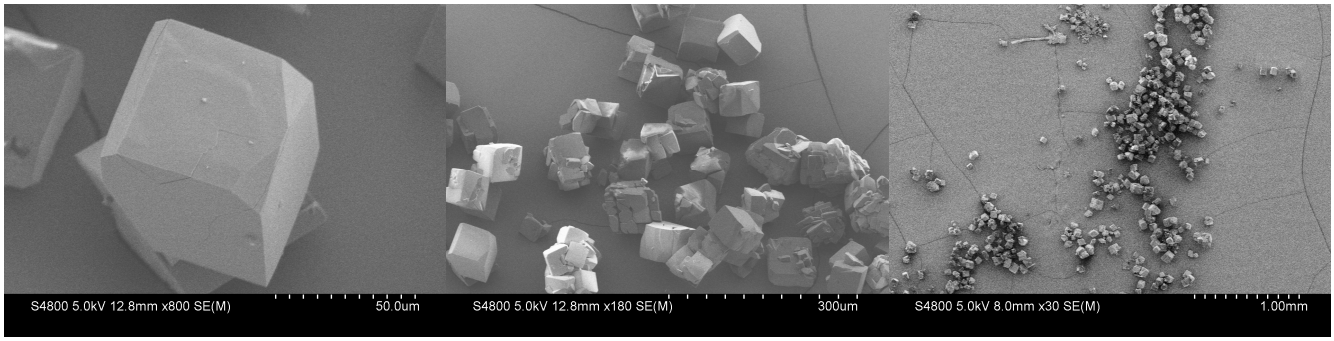

FIG S32
Cu(asp)bpe$_{0.5}$ (4):

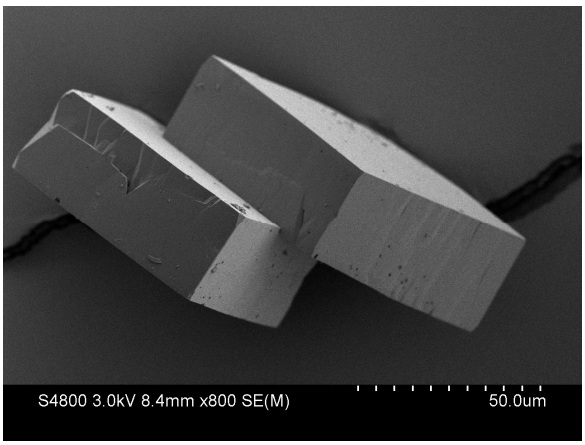

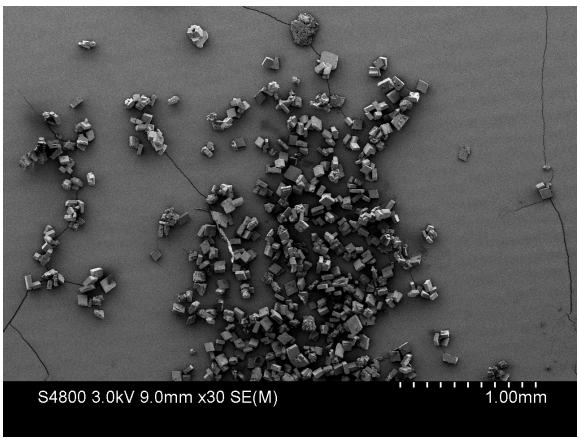

Simplified Structural Schematics

Topologically frameworks **1**, **3** and **4** are equivalent, being uni-nodal 5 connected networks, with the node in a square pyramidal environment. For compounds **1**, **3** and **4** a simplified structural representation is shown below (along each of the three axes). These idealized schematics are generated by extending the net from one copper node in each direction where there is a covalent connection (via aspartate or bipy bridging ligands) to an adjacent copper node. This produces the extended net consisting of a square pyramidal nodal environment with a bipy (or bpe) pillar bound in the apical position. The topology of all three materials can be expressed by the Schläfli symbol $4^4 \cdot 6^6$ (that signifies a five connected net with smallest constructing rings made up of 4 and 6 nodes), the second most common net for five connected nodes.[4] Using the three letter code system (proposed by O'Keeffe)[5] and determined using the Reticular Chemistry Structure Resource[6] for the square pyramid net structure that constructs the extended framework in **1**, **3** and **4** is represented as **sqp**, thus the full topological description is $4^4 \cdot 6^6$-sqp.

FIG S33:

Simplified view (left) down the b axis (cyan spheres = metal atoms at 50 % van der Waals radii). Blue struts represent direct covalent links between nodes. The unit cell is outlined in grey. The ac plane represents the 2D metal-aspartate layer with bipy (bpe) pillars set directly perpendicular. Right, molecular structure shown down the same axis for comparison.

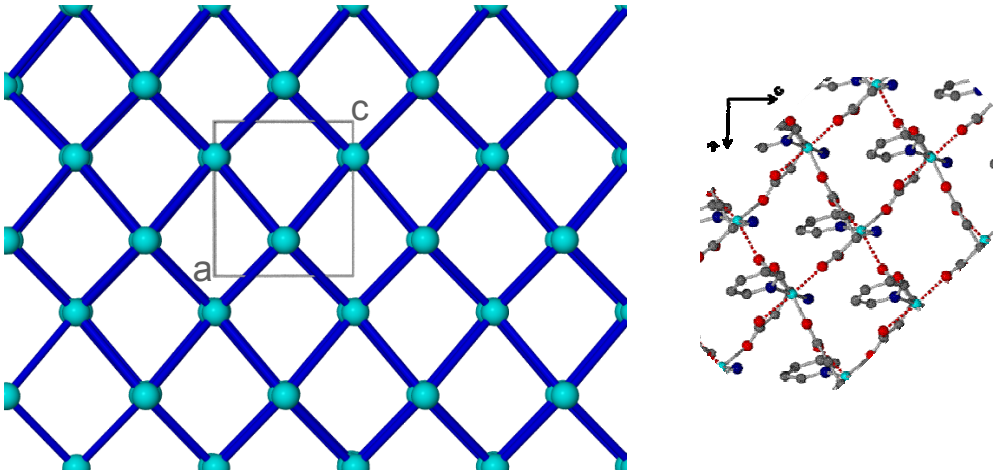

FIG S34

Simplified structural view down the c axis. Longer pillaring struts represent the bipy (or bpe) linker joining adjacent 2D layers. The unit cell is outlined in grey

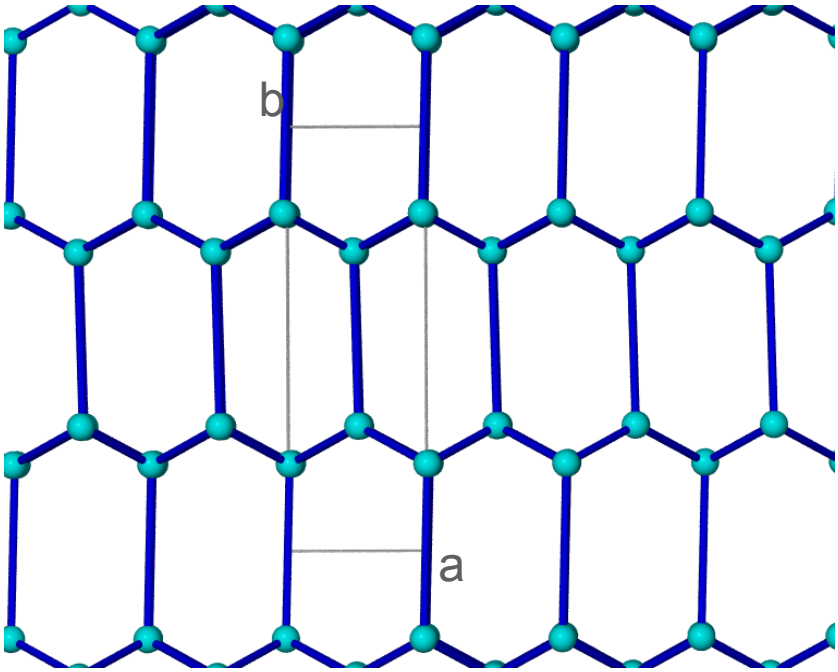

FIG S35

Simplified structural view (left) down the a axis. Longer pillaring struts represent the bipy (or bpe) linker joining adjacent 2D M(asp) layers. The unit cell is outlined in grey. Right, for comparison the molecular structure is shown down the same axis.

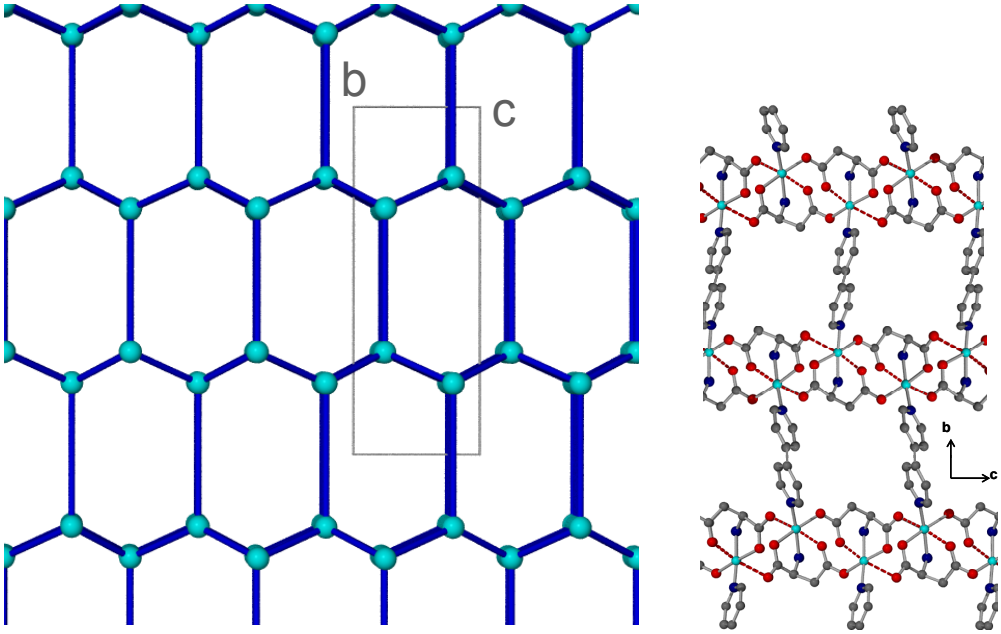

References:

1. R. Vaidhyanathan, D. Bradshaw, J.-N. Rebilly, J. P. Barrio, J. A. Gould, N. G. Berry and M. J. Rosseinsky, *Angew. Chem. Int. Ed. Engl.*, 2006, **45**, 6495 –6499.

2. Y. Permana, S. Shimazu, N. Ichikuni and T. Uematsu, *J. Mol. Catal. A*, 2004, **221**, 141-144.

3. G. K. Helmkamp and H. J. Lucas, *J. Am. Chem. Soc*, 1952, **70**, 951.

4. F. A. Mautner, M. A. S. Goher, H'a. E. Moustafa., M. A. M. Abu-Yossef, L. Öhrström, *Polyhedron*, 2007, 2703-2712..

5. O. Delgado Friedrichs, M. O'Keefe, O. M. Yaghi., Acta Cryst Sect. A., (2003), 22-27

6. The Reticular Chemistry Structure Resource by M. O'Keefe. http://rcsr.anu.edu.au/